Multiomics identifies unique modulators of calf muscle pathophysiology in peripheral artery disease and chronic kidney disease

Kyoungrae Kim[1], Trace Thome[1], Caroline Pass[1], Lauren Stone[1], Nicholas Vugman[1], Victoria Palzkill[1], Qingping Yang[1], Kerri A. O'Malley[2], Erik M. Anderson[2], Brian Fazzone[2], Feng Yue[3,5], Scott A. Berceli[2], Salvatore T. Scali[2], Terence E. Ryan[1,4,5,#]

[1]Department of Applied Physiology and Kinesiology

[2]Department of Surgery

[3]Department of Animal Sciences

[4]Center for Exercise Science

[5]Myology Institute

The University of Florida, Gainesville, FL, USA

Running Head: Multiomics in PAD and CKD

[#]Correspondence: Terence E. Ryan, PhD: 1864 Stadium Rd, Gainesville, FL, 32611. Tel: 352-294-1700 (office); email: ryant@ufl.edu; Twitter: @TerenceRyan_PhD

KEYWORDS: peripheral artery disease, renal, uremia, mitochondria, muscle

Manuscript word count: 3900

Abstract word count: 346

Running head character count: 25

Number of references: 68

Number of Grayscale figures: 0

Number of color figures: 7

Number of tables: 1

Table and Figure count: 8

ABSTRACT

BACKGROUND: Chronic kidney disease (CKD) has emerged as a significant risk factor that accelerates atherosclerosis, decreases muscle function, and increases the risk of amputation or death in patients with peripheral artery disease (PAD). However, the modulators underlying this exacerbated pathobiology are ill-defined. Recent work has demonstrated that uremic toxins are associated with limb amputation in PAD and have pathological effects in both the limb muscle and vasculature. Herein, we utilize multiomics to identify novel modulators of disease pathobiology in patients with PAD and CKD.

METHODS: A cross-sectional study enrolled four groups of participants: controls without PAD or CKD (n=28), patients with PAD only (n=46), patients with CKD only (n=31), and patients with both PAD and CKD (n=18). Both targeted (uremic toxins) and non-targeted metabolomics in plasma were performed using mass spectrometry. Calf muscle biopsies were used to measure histopathology, perform bulk and single-nucleus RNA sequencing (snRNAseq), and assess mitochondrial function. Differential gene and metabolite analyses, as well as pathway and gene set enrichment analyses were performed.

RESULTS: Patients with both PAD and CKD exhibited significantly lower calf muscle strength and smaller muscle fiber areas compared to controls and those with only PAD. Compared to controls, mitochondrial function was impaired in CKD patients, with or without PAD, but not in PAD patients without CKD.

Plasma metabolomics revealed substantial alterations in the metabolome of patients with CKD, with significant correlations observed between uremic toxins (e.g., kynurenine, indoxyl sulfate) and both muscle strength and mitochondrial function. RNA sequencing analyses identified downregulation of mitochondrial genes and pathways associated with protein translation in patients with both PAD and CKD. Single nucleus RNA sequencing further highlighted a mitochondrial deficiency in muscle fibers along with unique remodeling of fibro-adipogenic progenitor cells in patients with both PAD and CKD, with an increase in adipogenic cell populations.

CONCLUSIONS: CKD significantly exacerbates ischemic muscle pathology in PAD, as evidenced by diminished muscle strength, reduced mitochondrial function, and altered transcriptome profiles. The correlation between uremic toxins and muscle dysfunction suggests that targeting these metabolites may offer therapeutic potential for improving muscle health in PAD patients with CKD.

ABBREVIATIONS

CKD = chronic kidney disease; GFR = glomerular filtration rate; GSEA = gene set enrichment analysis; OXPHOS = oxidative phosphorylation; PAD = peripheral arterial disease; ROS = reactive oxygen species; snRNAseq = single nucleus RNA sequencing

INTRODUCTION

Peripheral arterial disease (PAD) is a condition characterized by atherosclerosis in the blood vessels of the lower extremities, affecting approximately 8-12 million Americans, and is a leading cause of cardiovascular mortality[1,2]. Common risk factors for PAD include age, smoking, diabetes, hypertension, and dyslipidemia. Notably, chronic kidney disease (CKD) is also strongly associated with PAD, contributing to the development of atherosclerosis, decreased muscle function, and an increased risk of amputation or death in patients with PAD[3-9]. Furthermore, CKD is linked to higher failure rates of both endovascular and open surgical revascularization procedures, which are commonly used in the management of PAD[3,10]. Recent work has reported a strong correlation between uremic metabolites—accumulating in CKD—and the risk of adverse limb events in patients with PAD[11]. Both PAD and CKD have been associated with skeletal muscle myopathy[12-24], suggesting that muscle tissue may be a key site where these two diseases intersect. Importantly, muscle function and exercise performance have

been established as strong predictors of morbidity and mortality in patients with PAD[13,15,25-27]. Despite these associations, the mechanisms underlying the exacerbated skeletal myopathy in patients with both PAD and CKD remain poorly understood. A deeper analysis could reveal novel targets for preventing or ameliorating muscle pathology in these patients. This cross-sectional study aimed to characterize the impact of PAD and CKD on skeletal muscle pathology by comparing calf muscle strength, mitochondrial function, and histopathology in four groups: 1) PAD patients, 2) PAD with CKD patients, 3) CKD patients, and 4) non-PAD and non-CKD controls. A multiomic approach, including bulk and single nucleus RNA sequencing of calf muscle specimens and both targeted and untargeted plasma metabolomics, was employed to identify novel regulators of skeletal muscle pathology

MATERIALS AND METHODS. Detailed descriptions of the materials and experimental procedures can be found in the Expanded Material and Methods section of the **Supplemental Material**. The data supporting the conclusions of this study are available from the corresponding author. A Major Resources Table is available in the **Supplemental Material**.

Study Population. This was a cross-sectional study involving participants without PAD or CKD, those with PAD only, those with CKD only, and those with both PAD and CKD. Participants were recruited through UF Health and the Malcom Randall VA Medical Centers in Gainesville, FL. This study was approved by the institutional review boards at the University of Florida and the Malcom Randall VA Medical Center (Protocol IRB201801553). All study procedures were carried out according to the Declaration of Helsinki and participants were fully informed about the research and informed consent was obtained. Patients with a normal ABI (greater than 0.9) or those with an abnormal ABI (less than 0.9) indicating a diagnosis of PAD with a Rutherford Stage between 3-5 set as inclusion criteria. Patients with non-atherosclerotic occlusive disease were excluded (acute limb ischemia, vasculitis, Buerger's disease, etc.). Inclusion criteria for CKD included an estimated glomerular filtration rate (eGFR) between 15 and 50 mL/min/1.73m^2 for greater than three months. Medical history, race, smoking history, and demographics were obtained by self-report. Co-existing medical conditions and medication usage was obtained through review of medical records. Non-PAD controls were recruited within the University of Florida Hospital System and Malcom Randall VA medical center and were free from peripheral vascular disease.

Calf muscle testing. A detailed description of analysis of calf muscle strength, muscle biopsy technique, mitochondrial function, muscle histopathology, and bulk and single nucleus RNA sequencing can be found on the **Supplemental Material**.

Plasma Metabolomics. A blood sample was obtained from a peripheral antebrachial vein using EDTA tubes and was subsequently centrifuged and plasma was frozen at -80°C until analysis. Sample underwent untargeted metabolomic analysis (Global Discovery platform) at a core laboratory using a well-validated Ultrahigh Performance Liquid Chromatography-Tandem Mass Spectroscopy (UPLC-MS/MS) platform (Metabolon, Inc.; Morrisville, NC, USA). The platform combines multiple sample preprocessing protocols and a comprehensive reference library, resulting in quantitative estimates of metabolite abundance covering a broad spectrum of chemical classes, including amino acids, carbohydrates, lipids, nucleotides, peptides and vitamins, xenobiotic substances, and pharmaceutical and food preservative compounds. A detailed description of the analytical protocol, metabolite identification, and normalization procedures is included in the Supplementary Methods. Samples were randomized across the platform run with quality control samples spaced evenly among the injections. Metabolite abundance was estimated from the area under the curve for annotated peaks in the mass spectrogram (mass spectral counts) and was normalized for batch and run day. Samples were also processed for targeted metabolomic analysis of kynurenine, tryptophan, 3-indoxyl sulfate, p-cresol sulfate (pCS), 4-ethylphenyl sulfate (4-EPS), 3-indolelactic acid, and 3-indolepropionic acid in which quantitative analysis was performed using standard curves for each metabolite.

Statistical analysis. Normality of data was tested with the Shapiro-Wilk test and inspection of QQ plots. Data involving comparisons of normally distributed data from groups were analyzed using a one-way ANOVA. Data involving comparisons of non-normally distributed data from groups were analyzed using a Kruskal-Wallis test. When appropriate, Tukey's posthoc testing was used to assess differences between groups. To assess relationships between two variables, Pearson correlation analysis was employed. Chi-Square analysis was used to determine differences in population proportions for relevant clinical characteristics. For bulk and snRNAseq, the Benjamini–Hochberg method was used to calculate false discovery rate corrected *P*-values. In all cases, $P < 0.05$ was considered statistically significant. All

statistical testing was conducted using R-studio, Python, or GraphPad Prism software (version 9.0). Data are presented as the mean ± standard deviation unless otherwise specified.

RESULTS

Patients with PAD and CKD have significantly lower calf muscle strength and myofiber areas. Fourty-six patients with PAD with normal kidney function, 18 patients with PAD and CKD, 31 patients with CKD only (no PAD), and 28 people with PAD or CKD were included in this study (N=123 total). The participant characteristics are shown in **Table 1**. Calf muscle (plantar flexors) strength was significantly lower in patients with PAD (P=0.0409), patients with CKD (P=0.0193), and patients with PAD and CKD (P<0.0001) when compared with controls that were free from PAD and CKD (**Figure 1A**). PAD patients with CKD had significantly lower calf muscle strength than PAD patients with normal kidney function (P=0.0103). After normalizing calf muscle strength to body weight, significant differences remained for PAD vs. PAD+CKD and control vs. PAD+CKD comparisons. Analysis of the mean myofiber cross sectional area demonstrated that PAD, CKD, and PAD+CKD groups had significantly smaller Type I and Type II myofibers compared to control participants (**Figure 1B,C**), however, the relative proportion fiber types was not significantly different (**Figure 1D**). Within the cohort, a significant correlation (Pearson r = 0.3160, P=0.0390) was observed between calf muscle strength and the mean myofiber area (**Figure 1E**). These findings reveal a clear deterioration in muscle function in PAD patients with CKD.

Calf muscle mitochondrial function is negatively impacted by CKD, but not PAD alone. High-resolution respirometry and fluorescence spectroscopy were used to assess muscle mitochondrial function in freshly permeabilized muscle fiber bundles using a creatine kinase clamp to perform a 'mitochondrial stress test" across a range of physiologically relevant energy demands (**Figure 2A**). Oxygen consumption (JO_2) was lower in patients with CKD and PAD+CKD, but nearly identical in patients with only PAD and control participants (**Figure 2B**). Quantification of the slope of oxygen consumption vs. energy demand (ΔG_{ATP}), termed OXPHOS conductance, represents the sensitivity of the mitochondrial system to respond to increases in energy demand. In this case, a higher OXPHOS conductance is interpreted as better mitochondrial function. OXPHOS conductance was not different between controls and PAD patients with normal kidney function (P=0.97), however CKD patients without PAD and PAD+CKD patients had

significantly lower OXPHOS conductance compared to controls (*P*=0.0123 and *P*=0.0054 respectively). PAD+CKD patients had significantly lower OXPHOS conductance than PAD patients without CKD (**Figure 2C**). Citrate synthase activity, a biomarker of mitochondrial content in skeletal muscle, was not significantly lower in CKD (*P*=0.095) and PAD+CKD (*P*=0.63) groups compared to controls (**Figure 2D**). Mitochondrial H_2O_2 emission was not significantly different between groups across the levels of energy demand (**Figure 2E**) or without energy demand (**Figure 2F**) when fueled by pyruvate/malate/octanoylcarnitine. When fueled with succinate in the absence of energy demand with or without inhibitors of the matrix antioxidant systems, PAD+CKD muscles had lower mitochondrial H_2O_2 emission than controls (**Figure 2G**). Succinate dehydrogenase (SHD) enzyme activity assessed histochemically on thin sections of muscle showed a lower SDH activity in CKD and PAD+CKD groups (**Figure 2H**).

CKD significantly alters the plasma metabolome. Next, we performed targeted metabolomics to quantify the absolute abundance of known uremic toxins including 3-indoxyl sulfate, p-cresol sulfate (pCS), 4-ethylphenyl sulfate (4-EPS), 3-indolelactic acid, 3-indolepropionic acid, kynurenine (L-Kyn), tryptophan (Trp), and the L-Kyn/Trp ratio in plasma of this cohort. As expected, CKD and PAD+CKD groups had significantly higher levels of all these uremic toxins (**Figure 3A**). No differences were found between controls and patients with PAD only. We also performed global untargeted metabolomics on the cohort which resulted in identification of 1557 metabolites/biochemicals, 1277 of which were identified in the compound library and 277 with unknown identity (**Figure 3B**). Principal component analysis revealed two relatively distinct clusters which separate the patients with and without CKD (**Figure 3C**). Compared to controls, patients with PAD had relatively similar plasma metabolomes with 99 differentially abundant metabolites (46 up and 53 down). In contrast, patients with CKD had 763 differentially abundant metabolites compared to controls (623 up and 140 down). Consistent with these findings, PAD+CKD patients had 578 differentially abundant metabolites (521 up and 57 down) compared to PAD patients. A heatmap with hierarchical clustering for all patients and metabolites is shown in **Figure 3D**. A Venn diagram showing the shared and distinct numbers of differentially abundant metabolites across comparisons is shown in **Figure 3E**. Pathway analysis revealed three main classes of metabolites were impacted by disease classification including “Uremic Toxins”, “Tissue Remodeling”, and Microbiome-related metabolites” (**Supplemental Figure 1**). The complete metabolomics dataset and pathway analysis can be found in Supplemental Datasets 1 and 2 respectively.

Skeletal muscle mitochondrial function and calf muscle strength are negatively correlated with tryptophan-derived uremic toxins. Previous studies have reported that tryptophan-derived uremic toxins, such as indoxyl sulfate and kynurenine, were negatively associated with muscle health and mitochondrial function[23,28-31]. Thus, we perform Pearson correlation analyses to determine if mitochondrial function (OXPHOS conductance) or muscle strength were related to these uremic toxins. Strikingly, kynurenine, L-Kyn/Trp ratio, and indoxyl sulfate had significant inverse correlations with both mitochondrial function (**Figure 4A**) and calf muscle strength (**Figure 4B**) in this cohort.

Whole muscle and single nucleus RNA sequencing identifies transcriptome changes in PAD patients with CKD. To understand how CKD impacts the skeletal muscle transcriptome, we performed bulk RNA sequencing on total RNA isolated from a portion of the gastrocnemius muscle biopsy of 88 patients. Gene expression was quantified for 24,871 genes. Comparing PAD to controls, 52 differentially expressed genes were detected (12 downregulated and 40 upregulated) (**Supplemental Figure 2A-D**). Comparing CKD to controls, 602 differentially expressed genes were detected (300 downregulated and 302 upregulated) (**Supplemental Figure 2E-H**). Comparing patients with PAD to those with PAD+CKD, partial least squares discriminant analysis (PLS-DA) showed two distinct clusters (**Figure 5A**). Patients with PAD+CKD had 361 differentially expressed genes from patients with only PAD (189 downregulated and 172 upregulated) (**Figure 5B**). GSEA in this comparison revealed that down regulated genes were significantly enriched in pathways related to “cellular respiration” and “oxidative phosphorylation”, whereas significantly upregulated genes were enriched in pathways related to “cytoplasmic translation”, “ribosome biogenesis”, and “rRNA processing” (**Figure 5C**). Full results of the DEG and GSEA analysis for each comparison can be found in Supplemental Dataset 3.

Because there are many cell types within skeletal muscle, we next used single nucleus RNA sequencing to enhance the resolution of analysis of calf muscle. 61,586 nuclei were analyzed from 20 PAD patients and 12 patients with PAD+CKD. Unsupervised clustering identified 14 clusters representing the major cell types expected in skeletal muscle (**Figure 5D**). Compared to PAD patients without CKD, PAD+CKD patients had fewer Type I myofiber nuclei and a higher proportion of nuclei that represented NMJ/regenerating myonuclei, fibro-adipogenic progenitor cells (FAPs), endothelial cells, and macrophages (**Figure 5E**). Top marker genes for each cell/nuclei type are shown in **Figure 5F**. DEG

229 analysis in the myofiber nuclei populations (**Figure 5G,H**) revealed a significant number of differentially
230 expressed genes within each cluster, however Type I myofiber nuclei had the largest number of DEGs.
231 With knowledge that bulk RNAseq GSEA analysis identified mitochondria as a downregulated biological
232 process, we generated a mitochondrial gene expression score which represents the overall
233 mitochondrial gene expression. This analysis confirmed all myonuclei populations in PAD+CKD muscles
234 displayed a mitochondrial deficiency, although Type I myofiber nuclei appeared to be most affected
235 (**Figure 5I**). GSEA analysis from myonuclei had common pathways related to "aerobic respiration" in the
236 downregulated DEGs (**Figure 5J**). Additional DEG, GSEA, and top marker genes for other cell types can be
237 found in Supplemental Dataset 4.

238

239 **Fibro-adipogenic progenitor (FAPs) cells are uniquely remodeled in muscle from patients with PAD**
240 **and CKD**. Next, we investigated how CKD impact FAPs, a resident mesenchymal stem cell population
241 that has been shown to be critical for muscle regeneration, were impacted by CKD in patients with PAD.
242 Subclustering of FAPs revealed eight distinct cell populations including pro-fibrotic, adipogenic, and
243 MME+ clusters[32] (**Figure 6A**). PAD patients with CKD had a higher abundance of adipocyte/adipogenic
244 FAPs (16% vs. 5.6%) and a unique population of ADAM12^{+} FAPs that was only present in PAD+CKD
245 (**Figure 6B**). We used the Palantir algorithm[33] to characterize differences in cell fate between PAD and
246 PAD+CKD FAPs. In patients with only PAD, a single terminate state representing the low abundance
247 adipocyte lineage was observed, whereas two clear terminal states were seen in PAD+CKD FAPs
248 (adipocyte and MME^{+}) along with a substantially higher differentiation potential in other populations
249 compared with FAPs from PAD patients (**Figure 6C**). Trajectory inference uncovered and additional
250 pathway for FAP differentiation in patients with PAD+CKD producing the ADAM12^{+} population (**Figure**
251 **6D**). Normalized gene expression showed the ADAM12^{+} FAP population was enriched for myokines IL6
252 and IGF1, whereas the pro-fibrotic FAPs displayed high expression of TGFB1 and COL1A1 (**Figure 6E**).
253 Expression of branch-specific genes along pseudotime are shown in **Figure 6F**. Other notable cell types
254 that displayed significant transcriptome and population differences in PAD+CKD included macrophages
255 (**Supplemental Figure 3**) and endothelial cells (**Supplemental Figure 4**).

256

257 **CKD influences intercellular communication in calf muscle from patients with PAD.** To explore how the
258 presence of CKD influences intercellular communication, we employed CellChat[34] to assess inferred

ligand-receptor interactions. Circle plots depicting the global intercellular communication are shown in **Figure 7A**, where the line width represents the communication strength. While the number of interactions was lower in PAD+CKD compared to PAD (2920 vs. 3552), the strength of those interactions was greater (**Figure 7B**). Comparisons of the major 'senders' and 'receivers' identified FAPs and adipocytes as the primary 'senders' whereas vascular populations including endothelial, lymphatic endothelial, and smooth muscle/pericyte cells were determined to be the major 'receivers' (**Figure 7C**). Significant signaling pathways between PAD and PAD+CKD were identified according to variations in information flow within inferred signaling networks (**Figure 7D**)

DISCUSSION

Patients with PAD often present with one or more comorbid conditions that worsen ischemic pathology and increase the risk of an adverse limb event. Recent studies have clearly demonstrated that CKD may be one of the strongest risk factors for poor outcomes in PAD[11,35]. In this cross-sectional study, we leveraged state-of-the-art multiomic analyses and mitochondrial and muscle function assessments to dissect how CKD impacts calf muscle pathophysiology in patients with PAD. Compared to non-PAD control with normal kidney function, patients with only PAD, patients with only CKD, and patients with both PAD and CKD had significantly weaker calf muscles and muscle fiber areas (Figure 1). Compared to patients with PAD, those with PAD and CKD were also significantly weaker and had smaller muscle fiber areas demonstrating that CKD exacerbates the ischemic myopathy in PAD. Skeletal muscle mitochondrial function was significantly impaired in patients with CKD only and those with PAD and CKD (Figure 2). Interestingly, no differences were observed between patients with PAD and the non-PAD controls. A significant negative correlation was found between the levels of indoxyl sulfate, L-Kynurenine, or the L-Kyn/Trp ratio and both mitochondrial function and muscle strength (Figure 4). This observation agrees with previous studies that reported similar associations in rodents with and without CKD [23,28-30], implicating uremic toxins as strong drivers of muscle impairment in CKD. These findings also agree with those of preclinical studies in which limb function of animals with CKD subjected to hindlimb ischemia was impaired compared to animals with normal kidney function subjected to hindlimb ischemia [11,30,36-38]. Mechanistically, recent studies have shown that the aryl hydrocarbon receptor is required for tryptophan-derived uremic toxins to impair skeletal muscle function and ischemic angiogenesis[11,30,38]. Beyond uremic toxins, tobacco smoking products also contain ligands that activate the aryl hydrocarbon receptor in skeletal muscle[39,40], namely 2,3,7,8-Tetrachlorodibenzodioxin (known

as TCDD), and smoking is considered the strongest risk factor for PAD suggesting this pathway could have a much broader impact of calf muscle pathophysiology in patients with PAD. In totality, these findings suggest that CKD induces muscle mitochondrial dysfunction in patients with and without PAD, potentially through mechanisms involving uremic toxins like indoxyl sulfate and kynurenines that activate the aryl hydrocarbon receptor.

Calf muscle mitochondrial OXPHOS was ~40% lower in patients with CKD than those without (Figure 2). This profound impact of CKD on skeletal muscle mitochondrial function and content aligns with previous studies[21,24,41-43]. In contrast, there were no differences between non-PAD controls and patients with PAD that had normal kidney function. This lack of difference in mitochondrial respiratory function is consistent with some previous studies[44-46], but not all[47-50] , that used similar methodologies. The lack of agreement across these studies may be due to modest sample sizes and differences in patient characteristics. Nonetheless, there is accumulating evidence that markers of mitochondrial content (mtDNA copy number, electron transport system complex abundance, citrate synthase activity, etc.) are increased in the calf muscle of patients with PAD[17,51,52]. This compensatory response is likely related to the hypoxia-induced energetic stress response that occurs within the calf muscles of PAD[17]. The striking impact of CKD on calf muscle mitochondrial health was also supported by the down regulation of mitochondrial gene expression observed in both bulk and single nucleus RNA sequencing analyses comparing PAD and PAD+CKD groups (Figure 5). In both diseases calf muscle mitochondrial function correlates with walking performance[24,52,53]. Further investigation is needed to determine whether interventions that improve or optimize calf muscle mitochondrial function can lead to improvements in walking performance in these patients.

Calf muscle from patients with PAD and CKD displayed a unique remodeling of a resident mesenchymal stem population called fibro-adipogenic progenitor cells (FAPs). These resident multipotent stem cells are located within the muscle interstitium where they have a heavy presence surrounding blood vessels. They have numerous differentiation paths with the two main fates being adipocytes or myofibroblasts[54]. Compared to PAD patients with normal kidney function, those with PAD and CKD had ~2.5-fold increase in adipocytes according to snRNAseq results. This accumulation of intramuscular adipose tissue is a form of myosteatosis which has been shown to impair muscle function[55,56] and regeneration from injury[57-59].

This phenotype has been observed independently in CKD[60] and PAD[61]. Considering that muscle function is strongly associated with mortality in PAD[13,15] and CKD[62], further studies are needed to determine if therapies the prevent or mitigate intramuscular adipose tissue in these conditions can improve muscle function and lower mortality risk.

Plasma metabolomics analyses revealed the wide-ranging impact on the plasma metabolome in patients with CKD (>500 differentially abundant biochemicals). In contrast, we found relatively few metabolites (99) that were differentially abundant between non-PAD controls and PAD patients. Only a few studies have examined the plasma metabolomes in patients with PAD[11,63-65], with the majority of studies reporting associations between amino acid metabolites, namely kynurenine and tryptophan, as well as indoles, and the risk of developing PAD or having adverse limb events[11,64,65]. The link between these uremic toxins and PAD risk may be indicative of the incidence of renal dysfunction in those study populations despite some studies excluding patients with diagnosed kidney disease. Alternatively, the source of kynurenines and indoles could be related to levels of systemic inflammation or dysregulation of the gut microbiome[66-68], both areas that have been underexplored in PAD. The highly overlapping plasma metabolomes between the non-PAD controls and patients with PAD may also be indicative of how well these groups were matched for co-morbid conditions, risk factors, and medication usage (Table 1). Additionally, the plasma metabolome in PAD is not likely to match the complex microenvironment within the affected limb where local metabolite alterations are presumed to be much greater than those reflected from a systemic plasma sample. Local sample collection from the diseased limb followed by subsequent metabolomic analyses could reveal the full impact of limb ischemia on metabolite exchange in tissues below of the occlusive lesion.

Given that our cohort of patients were restricted to moderate CKD (Stage 3b-4) and moderate-severe PAD (Rutherford Stage 3-5), our analyses may not be representative of the full spectrum of either disease. However, this design was chosen to enable deep phenotyping and multiomic analyses across the four groups. Additional studies should be performed to evaluate the reported relationships across the spectrum of both PAD and CKD. Although this patient cohort contained 39% female participants, we have not performed sex comparisons due to the relatively small sample sizes within each group for such a comparison. Future analyses of these data could be performed to begin understanding how biological

sex may alter the impact of CKD on PAD pathobiology. Additionally, while the control group was relatively well matched for clinical and physical characteristics, there were some comorbid conditions that were more prevalent in the PAD and CKD groups including hypertension and diabetes. It is important to note that these two conditions are among the strongest risk factors for developing CKD. This was a cross-sectional study design and longitudinal analyses were not performed. Thus, analyses exploring how specific outcomes change across time and whether they impact adverse limb events, morbidity, or mortality risk could not be performed. Despite these limitations, this study provides a robust and in-depth analysis of the skeletal myopathy in patients with PAD and CKD using physiological testing and multiomic analyses which identify pathways and processes that may have potential for interventional approaches that have promise to improve muscle function in these patients.

CONCLUSIONS

This study demonstrates that chronic kidney disease significantly worsens the ischemic limb myopathy in patients with PAD evidenced by lower calf muscle strength, muscle fiber sizes, and mitochondrial function. Multiomic analyses of calf muscle revealed a striking deficiency in myonuclear gene expression related to mitochondria and protein translation specifically in patients with both PAD and CKD, compared to those with only PAD. The significant correlation between plasma uremic toxin levels and both calf muscle strength and mitochondrial function suggests that therapeutic strategies aimed at reducing uremic toxins may hold promise for improving muscle health in patients with CKD.

Sources of Funding: This study was supported by National Institutes of Health (NIH) grants R01-HL149704 and HL171050 (T.E.R.). S.T.S. was supported by NIH grant R01HL148597. S.A.B. was supported by NIH grant R01DK119274. K.K. was supported by the American Heart Association grant POST903198. T.T. was supported by NIH grant F31-DK128920. V.R.P. was supported by the American Heart Association grant 24PRE1193999. C.P. was supported by the American Heart Association grant 24PRE1196311.

Disclosures: None.

Supplemental Material:

Expanded Materials and Methods

Supplemental Figures 1-4

Supplemental Dataset 1 (metabolomics).XLSX

Supplemental Dataset 2 (metabolomics pathway).XLSX

Supplemental Dataset 3 (bulk RNA).xlsx

Supplemental Dataset 4 (snRNA).xlsx

References

1. Ostchega Y, Paulose-Ram R, Dillon CF, Gu Q, Hughes JP. Prevalence of peripheral arterial disease and risk factors in persons aged 60 and older: data from the National Health and Nutrition Examination Survey 1999-2004. *J Am Geriatr Soc*. 2007;55:583-589. doi: 10.1111/j.1532-5415.2007.01123.x

2. Fowkes FG, Rudan D, Rudan I, Aboyans V, Denenberg JO, McDermott MM, Norman PE, Sampson UK, Williams LJ, Mensah GA, et al. Comparison of global estimates of prevalence and risk factors for peripheral artery disease in 2000 and 2010: a systematic review and analysis. *Lancet*. 2013;382:1329-1340. doi: 10.1016/S0140-6736(13)61249-0

3. Heideman PP, Rajebi MR, McKusick MA, Bjarnason H, Oderich GS, Friese JL, Fleming MD, Stockland AH, Harmsen WS, Mandrekar J, et al. Impact of Chronic Kidney Disease on Clinical Outcomes of Endovascular Treatment for Femoropopliteal Arterial Disease. *J Vasc Interv Radiol*. 2016;27:1204-1214. doi: 10.1016/j.jvir.2016.04.036

4. Kaminski MR, Raspovic A, McMahon LP, Lambert KA, Erbas B, Mount PF, Kerr PG, Landorf KB. Factors associated with foot ulceration and amputation in adults on dialysis: a cross-sectional observational study. *BMC Nephrol*. 2017;18:293. doi: 10.1186/s12882-017-0711-6

5. O'Hare AM, Sidawy AN, Feinglass J, Merine KM, Daley J, Khuri S, Henderson WG, Johansen KL. Influence of renal insufficiency on limb loss and mortality after initial lower extremity surgical revascularization. *J Vasc Surg*. 2004;39:709-716. doi: 10.1016/j.jvs.2003.11.038

6. Lacroix P, Aboyans V, Desormais I, Kowalsky T, Cambou JP, Constans J, Bura Riviere A, investigators C. Chronic kidney disease and the short-term risk of mortality and amputation in patients hospitalized for peripheral artery disease. *J Vasc Surg*. 2013;58:966-971. doi: 10.1016/j.jvs.2013.04.007

7. O'Hare AM, Bertenthal D, Shlipak MG, Sen S, Chren MM. Impact of renal insufficiency on mortality in advanced lower extremity peripheral arterial disease. *Journal of the American Society of Nephrology : JASN*. 2005;16:514-519. doi: 10.1681/ASN.2004050409

8. Pasqualini L, Schillaci G, Pirro M, Vaudo G, Siepi D, Innocente S, Ciuffetti G, Mannarino E. Renal dysfunction predicts long-term mortality in patients with lower extremity arterial disease. *J Intern Med*. 2007;262:668-677. doi: 10.1111/j.1365-2796.2007.01863.x

9. Liew YP, Bartholomew JR, Demirjian S, Michaels J, Schreiber MJ, Jr. Combined effect of chronic kidney disease and peripheral arterial disease on all-cause mortality in a high-risk population. *Clin J Am Soc Nephrol*. 2008;3:1084-1089. doi: 10.2215/CJN.04411007

10. Patel VI, Mukhopadhyay S, Guest JM, Conrad MF, Watkins MT, Kwolek CJ, LaMuraglia GM, Cambria RP. Impact of severe chronic kidney disease on outcomes of infrainguinal peripheral arterial intervention. *J Vasc Surg*. 2014;59:368-375. doi: 10.1016/j.jvs.2013.09.006

11. Arinze NV, Yin WQ, Lotfollahzadeh S, Napoleon MA, Richards S, Walker JA, Belghasem M, Ravid JD, Kamel MH, Whelan SA, et al. Tryptophan metabolites suppress the Wnt pathway and promote adverse limb events in chronic kidney disease. *J Clin Invest*. 2022;132. doi: ARTN e142260

10.1172/JCI142260

12. McDermott MM, Criqui MH, Greenland P, Guralnik JM, Liu K, Pearce WH, Taylor L, Chau CL, Celic L, Woolley C, et al. Leg strength in peripheral arterial disease: Associations with disease severity and lower-extremity performance. *Journal of Vascular Surgery*. 2004;39:523-530. doi: 10.1016/j.jvs.2003.08.038

13. Singh N, Liu K, Tian L, Criqui MH, Guralnik JM, Ferrucci L, Liao Y, McDermott MM. Leg strength predicts mortality in men but not in women with peripheral arterial disease. *J Vasc Surg*. 2010;52:624-631. doi: 10.1016/j.jvs.2010.03.066

14. Garg PK, Liu K, Ferrucci L, Guralnik JM, Criqui MH, Tian L, Sufit R, Nishida T, Tao HM, Liao YH, et al. Lower Extremity Nerve Function, Calf Skeletal Muscle Characteristics, and Functional Performance in Peripheral Arterial Disease. *J Am Geriatr Soc*. 2011;59:1855-1863. doi: 10.1111/j.1532-5415.2011.03600.x

15. McDermott MM, Liu K, Tian L, Guralnik JM, Criqui MH, Liao Y, Ferrucci L. Calf muscle characteristics, strength measures, and mortality in peripheral arterial disease: a longitudinal study. *J Am Coll Cardiol*. 2012;59:1159-1167. doi: 10.1016/j.jacc.2011.12.019

16. McDermott MM, Ferrucci L, Gonzalez-Freire M, Kosmac K, Leeuwenburgh C, Peterson CA, Saini S, Sufit R. Skeletal Muscle Pathology in Peripheral Artery Disease A Brief Review. *Arterioscl Throm Vas*. 2020;40:2577-2585. doi: 10.1161/Atvbaha.120.313831

17. Ferrucci L, Candia J, Ubaida-Mohien C, Lyaskov A, Banskota N, Leeuwenburgh C, Wohlgemuth S, Guralnik JM, Kaileh M, Zhang D, et al. Transcriptomic and Proteomic of Gastrocnemius

Muscle in Peripheral Artery Disease. *Circulation research*. 2023. doi: 10.1161/CIRCRESAHA.122.322325

18. John SG, Sigrist MK, Taal MW, McIntyre CW. Natural history of skeletal muscle mass changes in chronic kidney disease stage 4 and 5 patients: an observational study. *PLoS One*. 2013;8:e65372. doi: 10.1371/journal.pone.0065372

19. Tamaki M, Miyashita K, Wakino S, Mitsuishi M, Hayashi K, Itoh H. Chronic kidney disease reduces muscle mitochondria and exercise endurance and its exacerbation by dietary protein through inactivation of pyruvate dehydrogenase. *Kidney Int*. 2014;85:1330-1339. doi: 10.1038/ki.2013.473

20. Yokoi H, Yanagita M. Decrease of muscle volume in chronic kidney disease: the role of mitochondria in skeletal muscle. *Kidney Int*. 2014;85:1258-1260. doi: 10.1038/ki.2013.539

21. Gamboa JL, Roshanravan B, Towse T, Keller CA, Falck AM, Yu C, Frontera WR, Brown NJ, Ikizler TA. Skeletal Muscle Mitochondrial Dysfunction Is Present in Patients with CKD before Initiation of Maintenance Hemodialysis. *Clin J Am Soc Nephro*. 2020;15:926-936. doi: 10.2215/Cjn.10320819

22. Brightwell CR, Kulkarni AS, Paredes W, Zhang KH, Perkins JB, Gatlin KJ, Custodio M, Farooq H, Zaidi B, Pai RM, et al. Muscle fibrosis and maladaptation occur progressively in CKD and are rescued by dialysis. *Jci Insight*. 2021;6. doi: ARTN e150112

10.1172/jci.insight.150112

23. Thome T, Vugman NA, Stone LE, Wimberly K, Scali ST, Ryan TE. A tryptophan-derived uremic metabolite-Ahr-Pdk4 axis governs skeletal muscle mitochondrial energetics in chronic kidney disease. *JCI Insight*. 2024. doi: 10.1172/jci.insight.178372

24. Kestenbaum B, Gamboa J, Liu S, Ali AS, Shankland E, Jue T, Giulivi C, Smith LR, Himmelfarb J, de Boer IH, et al. Impaired skeletal muscle mitochondrial bioenergetics and physical performance in chronic kidney disease. *JCI Insight*. 2020;5. doi: 10.1172/jci.insight.133289

25. McDermott MM, Liu K, Ferrucci L, Tian L, Guralnik JM, Liao Y, Criqui MH. Decline in functional performance predicts later increased mobility loss and mortality in peripheral arterial disease. *J Am Coll Cardiol*. 2011;57:962-970. doi: 10.1016/j.jacc.2010.09.053

26. Jain A, Liu K, Ferrucci L, Criqui MH, Tian L, Guralnik JM, Tao H, McDermott MM. Declining walking impairment questionnaire scores are associated with subsequent increased mortality in peripheral artery disease. *J Am Coll Cardiol*. 2013;61:1820-1829. doi: 10.1016/j.jacc.2013.01.060

27. Leeper NJ, Myers J, Zhou M, Nead KT, Syed A, Kojima Y, Caceres RD, Cooke JP. Exercise capacity is the strongest predictor of mortality in patients with peripheral arterial disease. *J Vasc Surg*. 2013;57:728-733. doi: 10.1016/j.jvs.2012.07.051

28. Thome T, Kumar RA, Burke SK, Khattri RB, Salyers ZR, Kelley RC, Coleman MD, Christou DD, Hepple RT, Scali ST, et al. Impaired muscle mitochondrial energetics is associated with uremic metabolite accumulation in chronic kidney disease. *Jci Insight*. 2021;6.

29. Palzkill VR, Thome T, Murillo AL, Khattri RB, Ryan TE. Increasing plasma L-kynurenine impairs mitochondrial oxidative phosphorylation prior to the development of atrophy in murine skeletal muscle: A pilot study. *Frontiers in physiology*. 2022;13. doi: ARTN 992413

10.3389/fphys.2022.992413

30. Balestrieri N, Palzkill V, Pass C, Tan J, Salyers ZR, Moparthy C, Murillo A, Kim K, Thome T, Yang Q, et al. Activation of the Aryl Hydrocarbon Receptor in Muscle Exacerbates Ischemic Pathology in Chronic Kidney Disease. *Circulation research*. 2023;133:158-176. doi: 10.1161/CIRCRESAHA.123.322875

31. Hetherington-Rauth M, Johnson E, Migliavacca E, Parimi N, Langsetmo L, Hepple RT, Grzywinski Y, Corthesy J, Ryan TE, Ferrucci L, et al. Nutrient metabolites associated with low D3Cr muscle mass, strength, and physical performance in older men. *J Gerontol A Biol Sci Med Sci*. 2023. doi: 10.1093/gerona/glad217

32. Fitzgerald G, Turiel G, Gorski T, Soro-Arnaiz I, Zhang J, Casartelli NC, Masschelein E, Maffiuletti NA, Sutter R, Leunig M, et al. MME+ fibro-adipogenic progenitors are the dominant adipogenic population during fatty infiltration in human skeletal muscle. *Commun Biol*. 2023;6. doi: ARTN 111

10.1038/s42003-023-04504-y

33. Setty M, Kiseliovas V, Levine J, Gayoso A, Mazutis L, Pe'er D. Characterization of cell fate probabilities in single-cell data with Palantir. *Nature biotechnology*. 2019;37:451-460. doi: 10.1038/s41587-019-0068-4

34. Jin S, Guerrero-Juarez CF, Zhang L, Chang I, Ramos R, Kuan CH, Myung P, Plikus MV, Nie Q. Inference and analysis of cell-cell communication using CellChat. *Nat Commun*. 2021;12:1088. doi: 10.1038/s41467-021-21246-9

35. Amlani V, Ludwigs K, Rawshani A, Thuresson M, Falkenberg M, Smidfelt K, Nordanstig J. Major Adverse Limb Events in Patients Undergoing Revascularisation for Lower Limb Peripheral Arterial Disease: A Nationwide Observational Study(bigstar). *European journal of vascular and endovascular surgery : the official journal of the European Society for Vascular Surgery*. 2024. doi: 10.1016/j.ejvs.2024.07.041

36. Jacobi J, Porst M, Cordasic N, Namer B, Schmieder RE, Eckardt KU, Hilgers KF. Subtotal nephrectomy impairs ischemia-induced angiogenesis and hindlimb re-perfusion in rats. *Kidney Int*. 2006;69:2013-2021. doi: 10.1038/sj.ki.5000448

37. Berru FN, Gray SE, Thome T, Kumar RA, Salyers ZR, Coleman M, Dennis L, O'Malley K, Ferreira LF, Berceli SA, et al. Chronic kidney disease exacerbates ischemic limb myopathy in

mice via altered mitochondrial energetics. *Sci Rep*. 2019;9:15547. doi: 10.1038/s41598-019-52107-7

38. Palzkill VR, Tan J, Yang Q, Morcos J, Laitano O, Ryan TE. Deletion of the aryl hydrocarbon receptor in endothelial cells improves ischemic angiogenesis in chronic kidney disease. *Am J Physiol Heart Circ Physiol*. 2024;326:H44-H60. doi: 10.1152/ajpheart.00530.2023

39. Thome T, Miguez K, Willms AJ, Burke SK, Chandran V, de Souza AR, Fitzgerald LF, Baglole C, Anagnostou ME, Bourbeau J, et al. Chronic aryl hydrocarbon receptor activity phenocopies smoking-induced skeletal muscle impairment. *J Cachexia Sarcopenia Muscle*. 2022;13:589-604. doi: 10.1002/jcsm.12826

40. Fitzgerald LF, Lackey J, Moussa A, Shah SV, Castellanos AM, Khan S, Schonk M, Thome T, Salyers ZR, Jakkidi N, et al. Chronic aryl hydrocarbon receptor activity impairs muscle mitochondrial function with tobacco smoking. *J Cachexia Sarcopenia Muscle*. 2024;15:646-659. doi: 10.1002/jcsm.13439

41. Bittel DC, Bittel AJ, Varadhachary AS, Pietka T, Sinacore DR. Deficits in the Skeletal Muscle Transcriptome and Mitochondrial Coupling in Progressive Diabetes-Induced CKD Relate to Functional Decline. *Diabetes*. 2021;70:1130-1144. doi: 10.2337/db20-0688

42. Xu CQ, Kasimumali A, Guo XJ, Lu RH, Xie KW, Zhu ML, Qian YY, Chen XH, Pang HH, Wang Q, et al. Reduction of mitochondria and up regulation of pyruvate dehydrogenase kinase 4 of skeletal muscle in patients with chronic kidney disease. *Nephrology*. 2020;25:230-238. doi: 10.1111/nep.13606

43. Watson EL, Baker LA, Wilkinson TJ, Gould DW, Graham-Brown MPM, Major RW, Ashford RU, Philp A, Smith AC. Reductions in skeletal muscle mitochondrial mass are not restored following exercise training in patients with chronic kidney disease. *Faseb J*. 2020;34:1755-1767. doi: 10.1096/fj.201901936RR

44. Ryan TE, Yamaguchi DJ, Schmidt CA, Zeczycki TN, Shaikh SR, Brophy P, Green TD, Tarpey MD, Karnekar R, Goldberg EJ, et al. Extensive skeletal muscle cell mitochondriopathy distinguishes critical limb ischemia patients from claudicants. *JCI Insight*. 2018;3. doi: 10.1172/jci.insight.123235

45. Hart CR, Layec G, Trinity JD, Kwon OS, Zhao J, Reese VR, Gifford JR, Richardson RS. Increased skeletal muscle mitochondrial free radical production in peripheral arterial disease despite preserved mitochondrial respiratory capacity. *Exp Physiol*. 2018. doi: 10.1113/EP086905

46. Hart CR, Layec G, Trinity JD, Le Fur Y, Gifford JR, Clifton HL, Richardson RS. Oxygen availability and skeletal muscle oxidative capacity in patients with peripheral artery disease: implications from in vivo and in vitro assessments. *Am J Physiol-Heart C*. 2018;315:H897-H909. doi: 10.1152/ajpheart.00641.2017

47. Park SY, Pekas EJ, Anderson CP, Kambis TN, Mishra PK, Schieber MN, Wooden TK, Thompson JR, Kim KS, Pipinos, II. Impaired microcirculatory function, mitochondrial

respiration, and oxygen utilization in skeletal muscle of claudicating patients with peripheral artery disease. *Am J Physiol Heart Circ Physiol*. 2022;322:H867-H879. doi: 10.1152/ajpheart.00690.2021

48. Lindegard Pedersen B, Baekgaard N, Quistorff B. Mitochondrial dysfunction in calf muscles of patients with combined peripheral arterial disease and diabetes type 2. *International Angiology*. 2017;36:482-495. doi: 10.23736/S0392-9590.17.03824-X

49. Pipinos, II, Sharov VG, Shepard AD, Anagnostopoulos PV, Katsamouris A, Todor A, Filis KA, Sabbah HN. Abnormal mitochondrial respiration in skeletal muscle in patients with peripheral arterial disease. *J Vasc Surg*. 2003;38:827-832.

50. Pipinos, II, Judge AR, Zhu Z, Selsby JT, Swanson SA, Johanning JM, Baxter BT, Lynch TG, Dodd SL. Mitochondrial defects and oxidative damage in patients with peripheral arterial disease. *Free Radic Biol Med*. 2006;41:262-269. doi: 10.1016/j.freeradbiomed.2006.04.003

51. Picca A, Wohlgemuth SE, McDermott MM, Saini SK, Dayanidhi S, Zhang D, Xu S, Kosmac K, Tian L, Ferrucci L, et al. Mitochondrial Complex Abundance, Mitophagy Proteins, and Physical Performance in People With and Without Peripheral Artery Disease. *Journal of the American Heart Association*. 2023;12:e027088. doi: 10.1161/JAHA.122.027088

52. McDermott MM, Peterson CA, Sufit R, Ferrucci L, Guralnik JM, Kibbe MR, Polonsky TS, Tian L, Criqui MH, Zhao L, et al. Peripheral artery disease, calf skeletal muscle mitochondrial DNA copy number, and functional performance. *Vasc Med*. 2018:1358863X18765667. doi: 10.1177/1358863X18765667

53. Gonzalez-Freire M, Moore AZ, Peterson CA, Kosmac K, McDermott MM, Sufit RL, Guralnik JM, Polonsky T, Tian L, Kibbe MR, et al. Associations of Peripheral Artery Disease With Calf Skeletal Muscle Mitochondrial DNA Heteroplasmy. *Journal of the American Heart Association*. 2020;9:e015197. doi: 10.1161/JAHA.119.015197

54. Flores-Opazo M, Kopinke D, Helmbacher F, Fernandez-Verdejo R, Tunon-Suarez M, Lynch GS, Contreras O. Fibro-adipogenic progenitors in physiological adipogenesis and intermuscular adipose tissue remodeling. *Mol Aspects Med*. 2024;97:101277. doi: 10.1016/j.mam.2024.101277

55. Correa-de-Araujo R, Addison O, Miljkovic I, Goodpaster BH, Bergman BC, Clark RV, Elena JW, Esser KA, Ferrucci L, Harris-Love MO, et al. Myosteatosis in the Context of Skeletal Muscle Function Deficit: An Interdisciplinary Workshop at the National Institute on Aging. *Frontiers in physiology*. 2020;11. doi: ARTN 963

10.3389/fphys.2020.00963

56. Blitz NK, Collins KH, Shen KC, Schwartz K, Harris CA, Meyer GA. Infiltration of intramuscular adipose tissue impairs skeletal muscle contraction. *J Physiol-London*. 2020;598:2669-2683. doi: 10.1113/Jp279595

57. Norris AM, Appu AB, Johnson CD, Zhou LY, McKellar DW, Renault MA, Hammers D, Cosgrove BD, Kopinke D. Hedgehog signaling via its ligand DHH acts as cell fate determinant during skeletal muscle regeneration. *Nature Communications*. 2023;14. doi: ARTN 3766 10.1038/s41467-023-39506-1

58. Norris AM, Fierman KE, Campbell J, Pitale R, Shahraj M, Kopinke D. Studying intramuscular fat deposition and muscle regeneration: insights from a comparative analysis of mouse strains, injury models, and sex differences. *Skelet Muscle*. 2024;14:12. doi: 10.1186/s13395-024-00344-4

59. Joe AWB, Yi L, Natarajan A, Le Grand F, So L, Wang J, Rudnicki MA, Rossi FMV. Muscle injury activates resident fibro/adipogenic progenitors that facilitate myogenesis. *Nature cell biology*. 2010;12:153-U144. doi: 10.1038/ncb2015

60. Cheema B, Abas H, Smith B, O'Sullivan AJ, Chan M, Patwardhan A, Kelly J, Gillin A, Pang G, Lloyd B, et al. Investigation of skeletal muscle quantity and quality in end-stage renal disease. *Nephrology (Carlton)*. 2010;15:454-463. doi: 10.1111/j.1440-1797.2009.01261.x

61. Khattri RB, Kim K, Thome T, Salyers ZR, O'Malley KA, Berceli SA, Scali ST, Ryan TE. Unique Metabolomic Profile of Skeletal Muscle in Chronic Limb Threatening Ischemia. *Journal of Clinical Medicine*. 2021;10. doi: ARTN 548 10.3390/jcm10030548

62. Yang L, He Y, Li X. Physical function and all-cause mortality in patients with chronic kidney disease and end-stage renal disease: a systematic review and meta-analysis. *Int Urol Nephrol*. 2023;55:1219-1228. doi: 10.1007/s11255-022-03397-w

63. Ismaeel A, Franco ME, Lavado R, Papoutsi E, Casale GP, Fuglestad M, Mietus CJ, Haynatzki GR, Smith RS, Bohannon WT, et al. Altered Metabolomic Profile in Patients with Peripheral Artery Disease. *Journal of Clinical Medicine*. 2019;8. doi: ARTN 1463 10.3390/jcm8091463

64. Ho KJ, Ramirez JL, Kulkarni R, Harris KG, Helenowski I, Xiong L, Ozaki CK, Grenon SM. Plasma Gut Microbe-Derived Metabolites Associated with Peripheral Artery Disease and Major Adverse Cardiac Events. *Microorganisms*. 2022;10. doi: 10.3390/microorganisms10102065

65. Razquin C, Ruiz-Canela M, Toledo E, Clish CB, Guasch-Ferre M, Garcia-Gavilan JF, Wittenbecher C, Alonso-Gomez A, Fito M, Liang L, et al. Circulating Amino Acids and Risk of Peripheral Artery Disease in the PREDIMED Trial. *Int J Mol Sci*. 2022;24. doi: 10.3390/ijms24010270

66. Westbrook R, Chung T, Lovett J, Ward C, Joca H, Yang HL, Khadeer M, Tian J, Xue QL, Le AN, et al. Kynurenines link chronic inflammation to functional decline and physical frailty. *Jci Insight*. 2020;5. doi: ARTN 136091 10.1172/jci.insight.136091

67. Cervenka I, Agudelo LZ, Ruas JL. Kynurenines: Tryptophan's metabolites in exercise, inflammation, and mental health. *Science*. 2017;357. doi: 10.1126/science.aaf9794

68. Xue C, Li G, Zheng Q, Gu X, Shi Q, Su Y, Chu Q, Yuan X, Bao Z, Lu J, et al. Tryptophan metabolism in health and disease. *Cell Metab*. 2023;35:1304-1326. doi: 10.1016/j.cmet.2023.06.004

646

647

648

649

650

651

652

653

654

655 **TABLE 1: Participant Characteristics**

Physical Characteristics	Control (N=28)	PAD (N=46)	CKD (N=31)	PAD+CKD (N=18)	*P* value (χ^2 test or One-way ANOVA)
Mean age, y (SD)	64.4 (12.0)	64.5 (8.6)	62.1 (12.4)	65.5 (9.0)	0.6869
Female sex, n (%)	8 (28.6)	18 (39.1)	13 (41.9)	9 (50.0)	0.5111
Non-White, n (%)	4 (14.3)	10 (21.7)	12 (38.7)	6 (33.3)	0.1366
Non-Hispanic, n (%)	26 (92.9)	40 (87.0)	31 (100.0)	18 (100.0)	0.0835
BMI, kg/m^2 (SD)	29.1 (6.3)	27.6 (6.0)	30.0 (6.9)	28.3 (6.5)	0.4777
Disease Characteristics					
ABI (SD)	1.00 (0.08)	0.60 (0.26)	1.04 (0.16)	0.65 (0.24)	<0.0001
TBI (SD)	0.81 (0.17)	0.36 (0.21)	0.75 (0.15)	0.34 (0.23)	<0.0001
BUN, (mg/dL) (SD)	15.8 (5.8)	14.6 (5.2)	35.0 (18.0)	38.8 (25.6)	<0.0001
Creatinine, (mg/dL) (SD)	0.9 (0.2)	0.9 (0.2)	4.4 (2.5)	3.9 (3.7)	<0.0001

eGFR, (mL/min/1.73m^2) (SD)	73.9 (19.3)	70.2 (17.0)	26.0 (12.2)	30.1 (16.2)	<0.0001
Tobacco use					
Former smoker, n (%)	18 (66.7)	44 (95.7)	9 (30.0)	14 (77.8)	<0.0001
Current smoker, n (%)	7 (25.9)	13 (28.3)	1 (3.3)	6 (33.3)	0.0303
Medical History					
Diabetes type I or II, n (%)	9 (32.1)	20 (43.5)	16 (51.6)	14 (77.8)	0.0208
Hypertension, n (%)	18 (64.3)	38 (82.6)	30 (96.8)	17 (94.4)	0.0042
Hyperlipidemia, n (%)	17 (60.7)	35 (76.1)	18 (58.1)	15 (83.3)	0.1416
Coronary artery disease, n (%)	10 (35.7)	23 (50.0)	7 (22.6)	6 (33.3)	0.1028
Congestive heart failure, n (%)	6 (21.4)	9 (19.6)	9 (29.0)	7 (38.9)	0.3890
Medication used					
Aspirin, n (%)	15 (53.6)	35 (76.1)	13 (41.9)	12 (66.7)	0.0183
ACE inhibitor, n (%)	5 (17.9)	17 (37.0)	7 (22.6)	4 (22.2)	0.2581
Angiotensin receptor blocker, n (%)	4 (14.3)	8 (17.4)	8 (25.8)	7 (38.9)	0.1869
Statin, n (%)	21 (75.0)	37 (80.4)	22 (71.0)	17 (94.4)	0.2509
Cilostazol, n (%)	0 (0.0)	14 (30.4)	0 (0)	4 (22.2)	0.0006
Beta Blocker, n (%)	14 (50.0)	25 (54.3)	19 (61.3)	15 (83.3)	0.1201
Anticoagulant, n (%)	3 (10.7)	17 (37.0)	8 (25.8)	8 (44.4)	0.0430
Antiplatelet, n (%)	5 (17.9)	12 (26.1)	7 (22.6)	2 (11.1)	0.5764

Abbreviations: BMI = body mass index; ABI = ankle-brachial index; TBI = toe-brachial index; BUN = blood urea nitrogen; eGFR = estimated glomerular filtration rate; ACE = angiotensin converting enzyme

656

657

658

659

660

FIGURE LEGENDS

Figure 1. Calf muscle strength and muscle fiber area is lowest in patients with PAD and CKD. (**A**) Calf muscle strength in absolute and normalized to body weight (n=102). (**B**) Representative immunofluorescence images of gastrocnemius muscle biopsies with fiber types and sizes labeled. (**C**) Violin plots showing the cross-sectional areas of Type I (n=8816 myofibers) and Type II (n=8395) myofibers in each patient group (n=63 patients). (**D**) Quantification of the percentage of Type I fibers (n=63 patients). (E) Pearson correlation between calf muscle strength and mean myofiber area (both Type I and II myofibers) (n=43 patients). Panel A was analyzed using a Kruskal-Wallis Test with Dunn's test for pairwise comparisons. Panel C and D were analyzed using a one-way ANOVA with Tukey's post hoc testing. Error bars represent the standard deviation.

Figure 2. Skeletal muscle mitochondrial function is significantly impaired in patients with CKD and PAD+CKD. (**A**) Graphical depiction of mitochondrial analyses using permeabilized myofibers. (**B**) Relationship between oxygen consumption (JO_2) and energy demand (ΔG_{ATP}) when mitochondria were fueled with pyruvate, malate, and octanoylcarnitine. (**C**) Quantification of the conductance (the slope of JO_2 and ΔG_{ATP} relationship) (n=86 patients). (**D**) Citrate synthase activity in gastrocnemius muscle (n= 81 patients). (**E**) Relationship between mitochondrial hydrogen peroxide production (JH_2O_2) and energy demand (ΔG_{ATP}) when mitochondria were fueled with pyruvate, malate, and octanoylcarnitin. (**F**) Quantification of JH_2O_2 under state 2 (no energy demand) conditions (n=82 patients). (**G**) Quantification of JH_2O_2 with mitochondrial fueled with succinate followed by inhibition of the matrix antioxidant systems (with AF/BCNU) (n=85 patients). Analyzed via two-way ANOVA with Tukey's post hoc. (**H**) Representative images and quantification of succinate dehydrogenase (SDH) activity in muscle sections (n= patients.

Panels C, D, F, and H were analyzed with a one-way ANOVA with Tukey's post hoc. Error bars represent the standard deviation.

Figure 3. CKD profoundly impacts the plasma metabolome independent of PAD. (**A**) Targeted plasma metabolomic quantification of uremic toxins (n=97 patients). Analysis done using one-way ANOVA with Tukey's post hoc. (**B**) Graphic of experimental design and overall metabolite detection for untargeted (global) metabolomics in patient plasma. (**C**) Principal component analysis demonstrates separation between CKD and non-CKD patients, independent of PAD. (**D**) A heatmap with hierarchical clustering of metabolites and patients. (**E**) Venn diagram showing significant metabolite differences across group comparisons. Error bars represent the standard deviation.

Figure 4. Uremic toxin levels have an inverse relationship with calf muscle mitochondrial function and strength. (**A**) Pearson correlations between OXPHOS conductance and L-Kynurenine, L-Kyn/Trp ratio,

and indoxyl sulfate levels (n=81 patients). (**B**) Pearson correlations between calf muscle strength and L-Kynurenine, L-Kyn/Trp ratio, and indoxyl sulfate levels (n=72 patients). Statistical analyses performed using two-tailed Pearson correlation.

Figure 5. Whole muscle and single nucleus RNA sequencing identify mitochondrial deficiency and cytoplasmic translation defects in patients with PAD+CKD. (**A**) RNA sequencing on total RNA from the gastrocnemius was performed (n=88 patients). Partial least squares discriminant analysis (PLS-DA) revealed clear separation between PAD and PAD+CKD patients. (**B**) Volcano plot of gene expression shows differentially expressed genes in PAD and PAD+CKD patients. (**C**) Gene set enrichment analysis in significantly upregulated and downregulated genes between PAD and PAD+CKD patients. (**D**) Single nucleus RNA sequencing was performed on gastrocnemius muscle specimens from 20 PAD and 12 PAD+CKD patients. UMAPs presented by group and by cell types are shown. (**E**) Percentage of nuclei within each cluster determined by group. (**F**) Dotplots of the top 4 marker genes for each cell type. (**G**) UMAPs of the subclustering of myofiber nuclei by group and type. (**H**) Venn diagrams shown differentially expressed genes by myonuclei type. (**I**) UMAPs showing the mitochondrial gene module score for each nuclei demonstrated the mitochondrial deficiency in PAD+CKD muscles. (**J**) Gene set enrichment analysis results for myonuclei populations. The x-axis is the normalized enrichment score and the values for each bar are the adjusted *P*-values.

Figure 6. Fibro-adipogenic progenitor cells are uniquely remodeled in muscles from patients with PAD+CKD. (**A**) UMAPs of the subclustering of FAPs presented by group and by subpopulation type are shown. (**B**) Donut plots showing the abundance of subpopulations of FAPs in both groups. (**C**) Ranked significant ligand-receptor communications for relative information flow between $AHR^{fl/fl}$ and AHR^{mKO} muscles. (**D**) Trajectory inference in FAPs showed three distinct fates in PAD+CKD. (**E**) Feature plots showing normalized gene expression levels for inflammatory, pro-fibrotic, and adipogenic genes. (**F**) Gene expression changes across those three fates across pseudotime for both groups.

Figure 7. CellChat analysis predicts changes in intercellular communication of PAD+CKD patients. (**A**) Circle plots showing the overall intercellular communication occurring in non-PAD and PAD. Circle sizes represent the number of cells and edge width represents communication probability. (**B**) Comparison of outgoing and incoming interaction strengths for all cells type in non-PAD and PAD. (**C**) Ranked significant ligand-receptor communications for relative information flow between non-PAD and PAD muscles. (**D**) Circle plots for FGF signaling communication in non-PAD and PAD.

NOVELTY AND SIGNIFICANCE

What is known?

- Peripheral artery disease (PAD) patients with chronic kidney disease (CKD) have poorer health outcomes and increased risk for adverse limb events and mortality compared with patients with normal kidney function.
- The accumulation of uremic toxins in CKD have been associated with adverse limb events in patients that have PAD.

What new information does this article contribute?

- Patients with PAD and CKD have significantly lower calf muscle strength, muscle fiber size, and mitochondrial function compared to PAD patients with normal kidney function.
- CKD, but not PAD alone, has a significant impact on the plasma metabolome.
- Uremic toxins such as indoxyl sulfate and L-Kynurenine have significant inverse relationships with calf muscle strength and mitochondrial function.
- Bulk and single nucleus RNA sequencing reveals a mitochondrial deficiency in myofibers and pro-fibrotic/pro-adipogenic differentiation states of fibro-adipogenic progenitor cells in patients with PAD and CKD.

There is overwhelming evidence that PAD patients with CKD have significantly higher risk of major adverse limb events and death compared to PAD patients without CKD. Moreover, having CKD increases the likelihood that endovascular and open revascularization procedures fail in patients with PAD. Skeletal muscle pathologies have been shown to play important roles in both PAD and CKD

independently. Because skeletal muscle function is a strong predictor of morbidity and mortality, it is important to understand how CKD exacerbates the myopathy of PAD to improve medical management in these patients. In a cohort of 123 patients, calf muscle strength was lowest in PAD patients with CKD, although both those PAD and CKD alone were also significantly weaker than non-PAD and non-CKD controls. Muscle fiber atrophy was also evident and muscle fiber size correlated with calf muscle strength. Using calf muscle biopsies, we found that mitochondrial function was significantly impaired in patients with CKD and those with PAD+CKD. Significant inverse correlations were found between uremic toxins and muscle strength and mitochondrial function. Bulk and single nucleus RNA sequencing revealed the wide-ranging impact of CKD on the muscle transcriptome in patients with PAD. In summary, this study establishes CKD as a major driver of skeletal muscle pathology in patients with PAD.

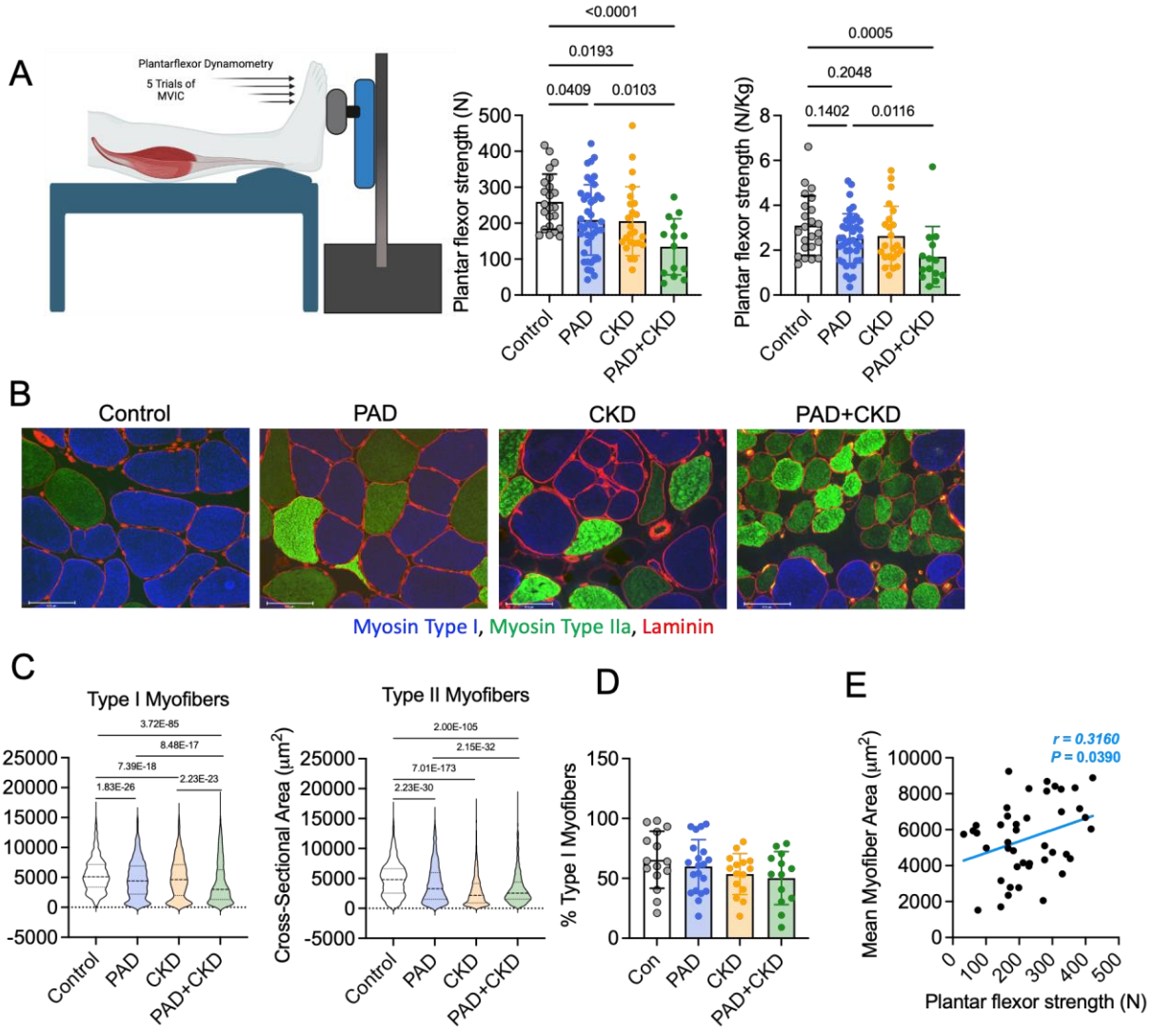

Figure 1. Calf muscle strength and muscle fiber area is lowest in patients with PAD and CKD. (**A**) Calf muscle strength in absolute and normalized to body weight (n=102). (**B**) Representative immunofluorescence images of gastrocnemius muscle biopsies with fiber types and sizes labeled. (**C**) Violin plots showing the cross-sectional areas of Type I (n=8816 myofibers) and Type II (n=8395) myofibers in each patient group (n=63 patients). (**D**) Quantification of the percentage of Type I fibers (n=63 patients). (E) Pearson correlation between calf muscle strength and mean myofiber area (both Type I and II myofibers) (n=43 patients). Panel A was analyzed using a Kruskal-Wallis Test with Dunn's test for pairwise comparisons. Panel C and D were analyzed using a one-way ANOVA with Tukey's post hoc testing. Error bars represent the standard deviation.

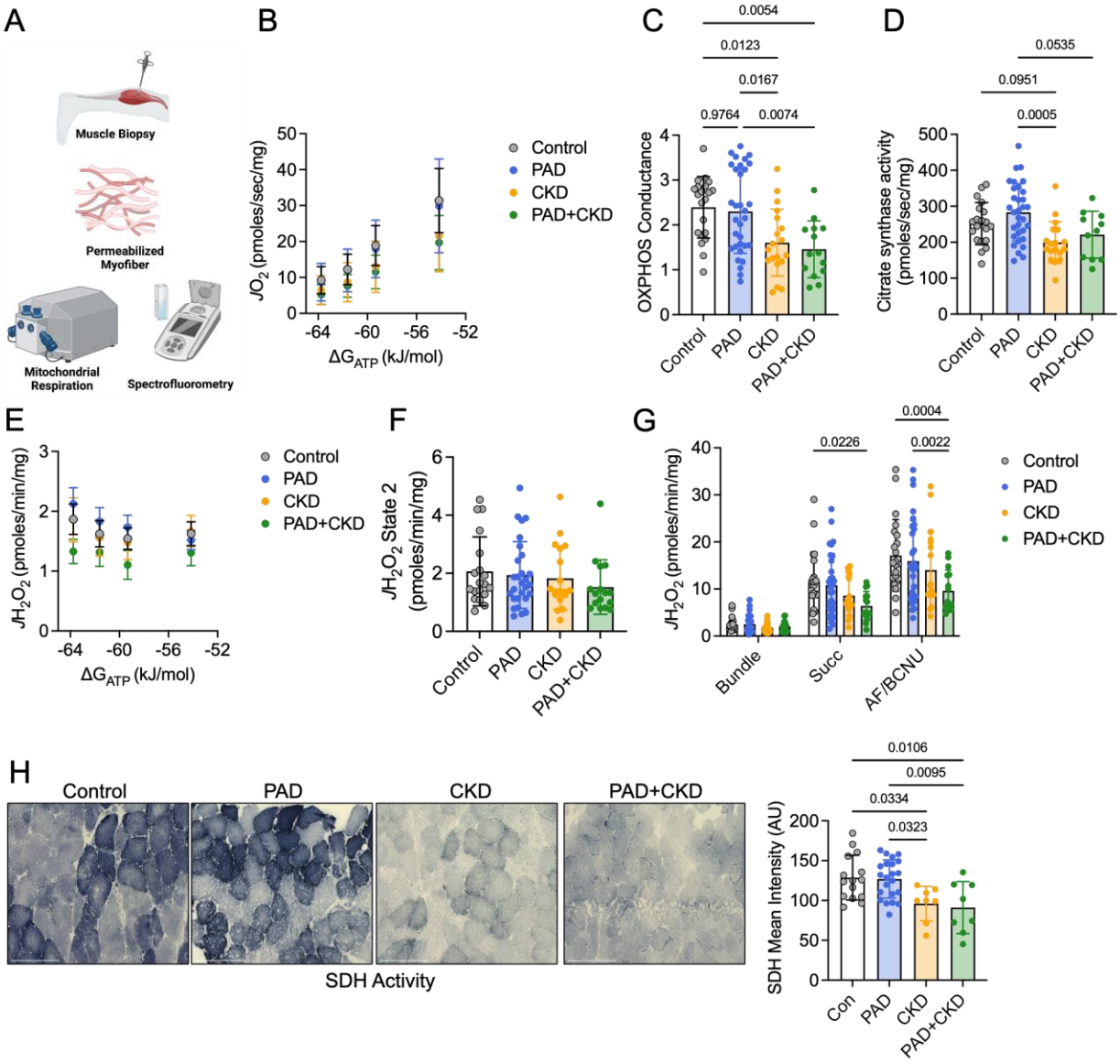

Figure 2. Skeletal muscle mitochondrial function is significantly impaired in patients with CKD and PAD+CKD. (**A**) Graphical depiction of mitochondrial analyses using permeabilized myofibers. (**B**) Relationship between oxygen consumption (JO_2) and energy demand (ΔG_{ATP}) when mitochondria were fueled with pyruvate, malate, and octanoylcarnitine. (**C**) Quantification of the conductance (the slope of JO_2 and ΔG_{ATP} relationship) (n=86 patients). (**D**) Citrate synthase activity in gastrocnemius muscle (n= 81 patients). (**E**) Relationship between mitochondrial hydrogen peroxide production (JH_2O_2) and energy demand (ΔG_{ATP}) when mitochondria were fueled with pyruvate, malate, and octanoylcarnitin. (**F**)

807 Quantification of JH_2O_2 under state 2 (no energy demand) conditions (n=82 patients). (**G**) Quantification
808 of JH_2O_2 with mitochondrial fueled with succinate followed by inhibition of the matrix antioxidant
809 systems (with AF/BCNU) (n=85 patients). Analyzed via two-way ANOVA with Tukey's post hoc. (**H**)
810 Representative images and quantification of succinate dehydrogenase (SDH) activity in muscle sections
811 (n= patients.

812 Panels C, D, F, and H were analyzed with a one-way ANOVA with Tukey's post hoc. Error bars represent
813 the standard deviation.

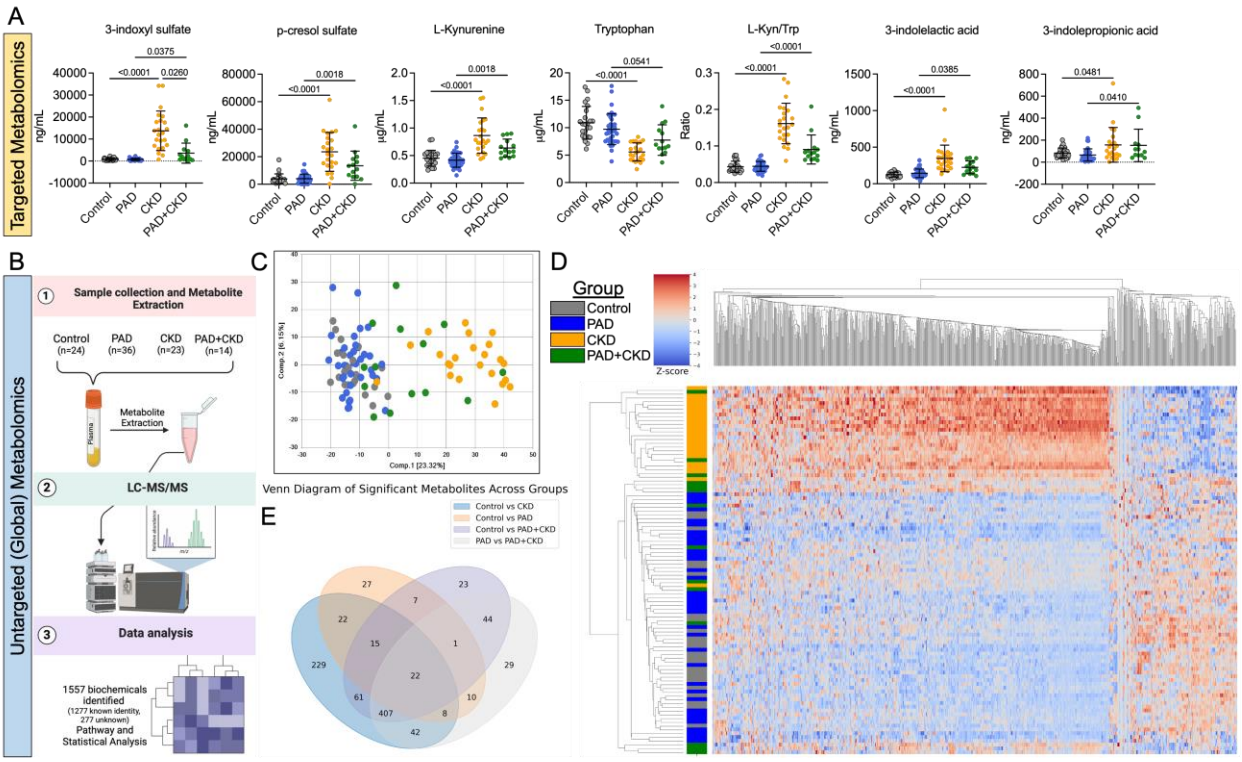

814

815

816 **Figure 3. CKD profoundly impacts the plasma metabolome independent of PAD.** (**A**) Targeted plasma
817 metabolomic quantification of uremic toxins (n=97 patients). Analysis done using one-way ANOVA with
818 Tukey's post hoc. (**B**) Graphic of experimental design and overall metabolite detection for untargeted
819 (global) metabolomics in patient plasma. (**C**) Principal component analysis demonstrates separation
820 between CKD and non-CKD patients, independent of PAD. (**D**) A heatmap with hierarchical clustering of
821 metabolites and patients. (**E**) Venn diagram showing significant metabolite differences across group
822 comparisons. Error bars represent the standard deviation.

823

824

825

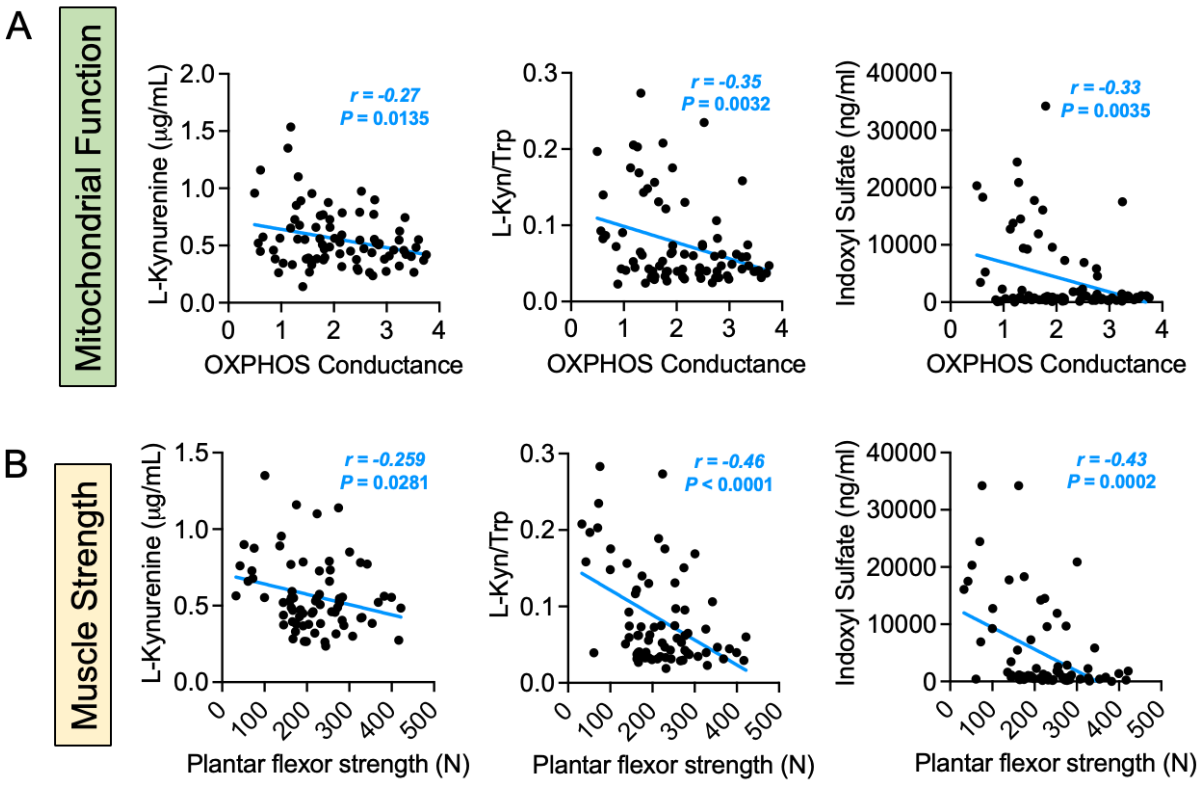

Figure 4. Uremic toxin levels have an inverse relationship with calf muscle mitochondrial function and strength. (**A**) Pearson correlations between OXPHOS conductance and L-Kynurenine, L-Kyn/Trp ratio, and indoxyl sulfate levels (n=81 patients). (**B**) Pearson correlations between calf muscle strength and L-Kynurenine, L-Kyn/Trp ratio, and indoxyl sulfate levels (n=72 patients). Statistical analyses performed using two-tailed Pearson correlation.

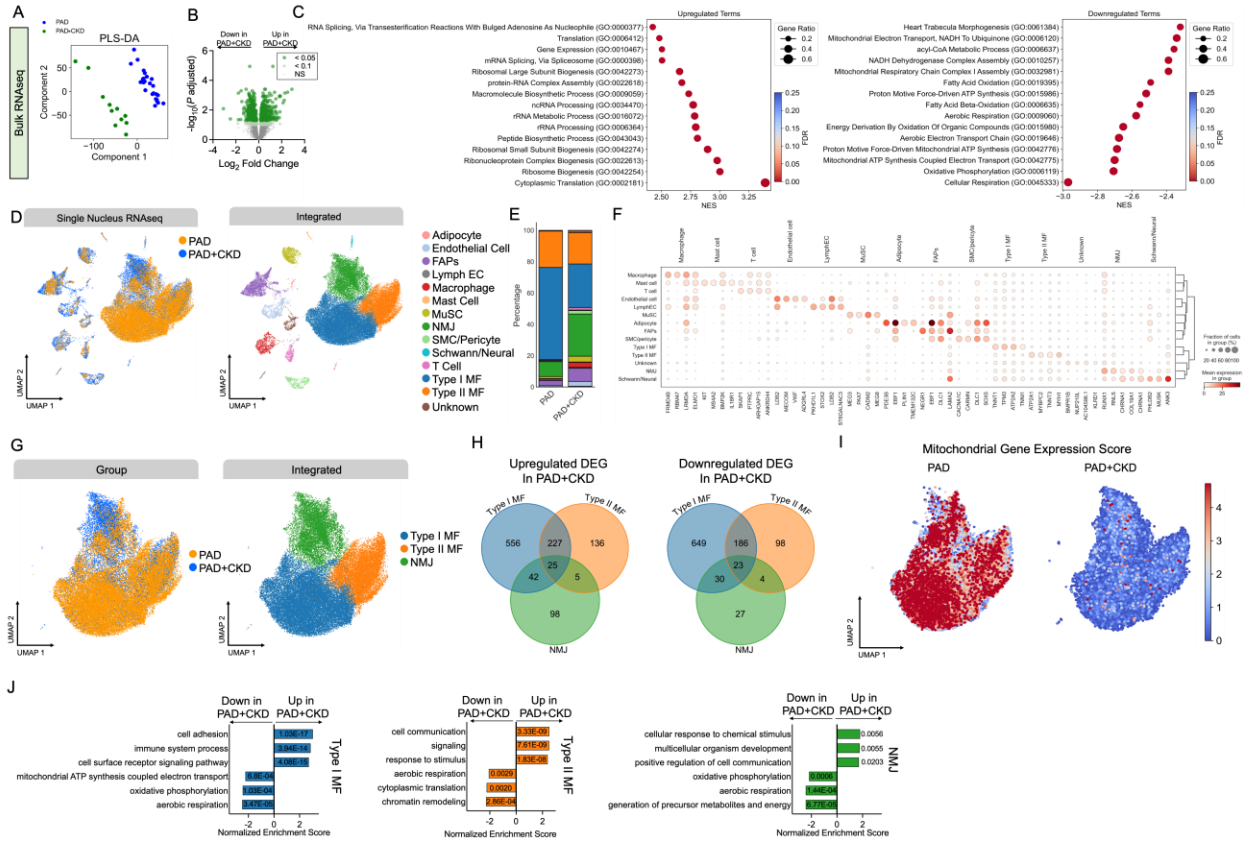

Figure 5. Whole muscle and single nucleus RNA sequencing identify mitochondrial deficiency and cytoplasmic translation defects in patients with PAD+CKD. (**A**) RNA sequencing on total RNA from the gastrocnemius was performed (n=88 patients). Partial least squares discriminant analysis (PLS-DA) revealed clear separation between PAD and PAD+CKD patients. (**B**) Volcano plot of gene expression shows differentially expressed genes in PAD and PAD+CKD patients. (**C**) Gene set enrichment analysis in significantly upregulated and downregulated genes between PAD and PAD+CKD patients. (**D**) Single nucleus RNA sequencing was performed on gastrocnemius muscle specimens from 20 PAD and 12 PAD+CKD patients. UMAPs presented by group and by cell types are shown. (**E**) Percentage of nuclei within each cluster determined by group. (**F**) Dotplots of the top 4 marker genes for each cell type. (**G**) UMAPs of the subclustering of myofiber nuclei by group and type. (**H**) Venn diagrams shown differentially expressed genes by myonuclei type. (**I**) UMAPs showing the mitochondrial gene module score for each nuclei demonstrated the mitochondrial deficiency in PAD+CKD muscles. (**J**) Gene set enrichment analysis results for myonuclei populations. The x-axis is the normalized enrichment score and the values for each bar are the adjusted *P*-values.

881

882

883

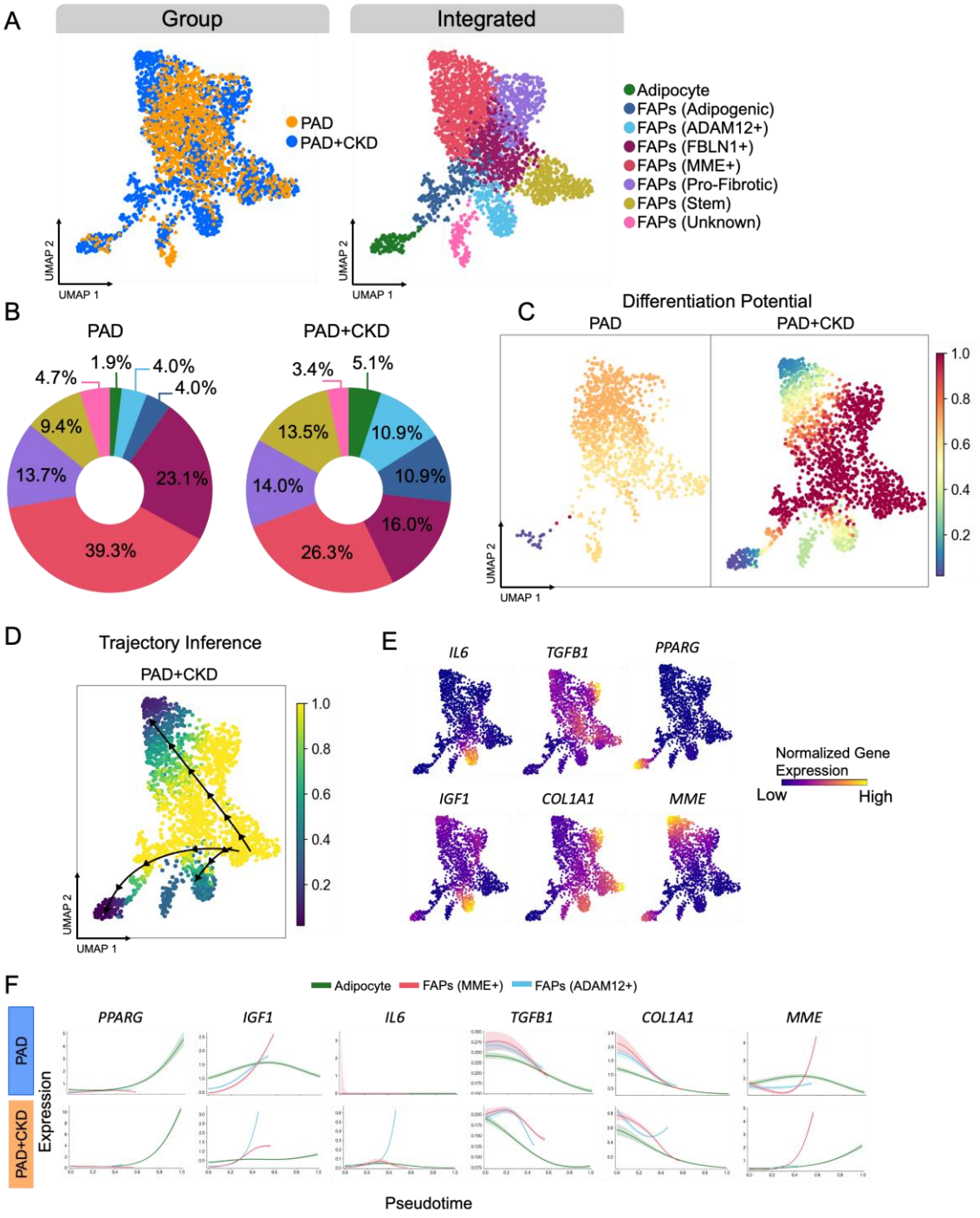

884

885 **Figure 6. Fibro-adipogenic progenitor cells are uniquely remodeled in muscles from patients with**
886 **PAD+CKD.** (**A**) UMAPs of the subclustering of FAPs presented by group and by subpopulation type are

887 shown. (**B**) Donut plots showing the abundance of subpopulations of FAPs in both groups. (**C**) Ranked
888 significant ligand-receptor communications for relative information flow between $AHR^{fl/fl}$ and AHR^{mKO}
889 muscles. (**D**) Trajectory inference in FAPs showed three distinct fates in PAD+CKD. (**E**) Feature plots
890 showing normalized gene expression levels for inflammatory, pro-fibrotic, and adipogenic genes. (**F**)
891 Gene expression changes across those three fates across pseudotime for both groups.

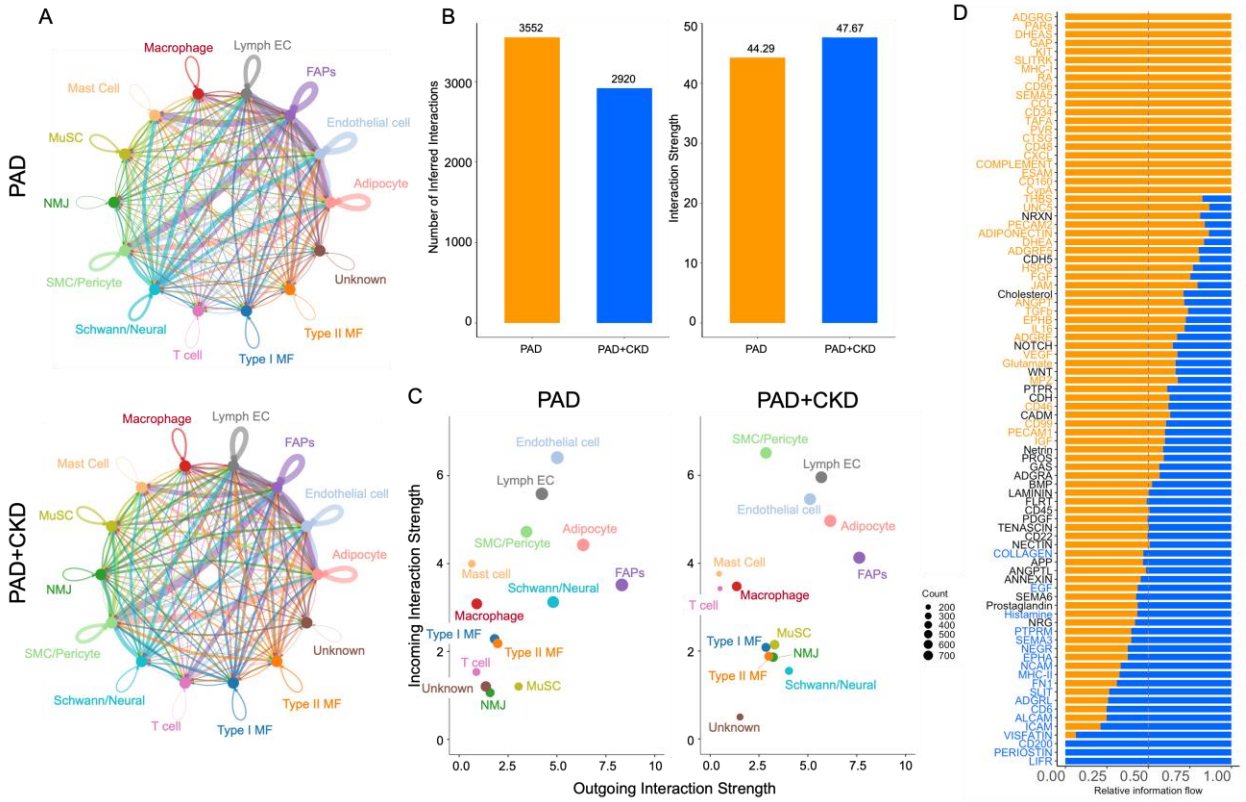

892

893

894 **Figure 7. CellChat analysis predicts changes in intercellular communication of PAD+CKD patients.** (**A**)
895 Circle plots showing the overall intercellular communication occurring in non-PAD and PAD. Circle sizes
896 represent the number of cells and edge width represents communication probability. (**B**) Comparison of
897 outgoing and incoming interaction strengths for all cells type in non-PAD and PAD. (**C**) Ranked significant
898 ligand-receptor communications for relative information flow between non-PAD and PAD muscles. (**D**)
899 Circle plots for FGF signaling communication in non-PAD and PAD.

900